SVPWM Inverter for Induction Motor

Sreeranjini C Nair[1] Jisha Kuruvilla P[2] Annie P Oommen[3]
[1]Student [2]Assistant Professor [3]Professor
[1,2,3]Mar Athanasius College of Engineering

Abstract— the induction machines are widely used in a wide variety of applications. The dynamic simulation is one of the key steps in the validation of the design process of the motor drive system, which eliminates the designing mistakes and the resulting errors in the prototype construction and testing. Variable voltage and frequency supply to ac drives is invariably obtained from a three-phase voltage source inverter (VSI). A number of Pulse width modulation (PWM) scheme is used to obtain variable voltage and frequency supply. The most widely used PWM schemes for three-phase VSI are carrier-based sinusoidal PWM and space vector PWM (SVPWM). There is an increasing trend of using space vector PWM (SVPWM) because of their easier digital realisation and better dc bus utilisation. Firstly, model of a three-phase VSI is discussed based on space vector representation. And the simulation model of SVPWM inverter is obtained using MATLAB/SIMULINK. The prototype of 3 phase SVPWM bridge inverter is setup and gate pulses are obtained from Arduino Mega2560. Also this paper presents MATLAB /SIMULINK implementation of an induction machine using dq0 axis transformations of the stator and rotor variables in the arbitrary reference frame.

Key words: SVPWM Inverter, MATLAB/SIMULINK

I. INTRODUCTION

Three phase Induction Motors are the most extensively used machines in various electrical drives due to their reliability, ruggedness and relatively lower cost. Around 70% of all industry loads on a utility are represented by IMs. Due to rapidly increasing electricity prices, it becomes of prime penchant for researchers that awareness be paid for efficient optimization of IMs. Generally for rated speed and torque, IM show high efficiency. However, at light loads considerable reduction in motor efficiency due is observed due to increase in iron losses. Therefore to optimize efficiency of motor at partial loads, it is essential to obtain such flux levels that maintain a balance between iron and copper losses [1]. The supply for the 3 phase induction motor is obtained using a 3 phase bridge inverter. The Major drawback of conventional bridge inverter is that its output contains all odd harmonics except the triplen harmonics. It will deteriorate the performance, quality of the system. Presence of harmonics cause malfunction in the microprocessor based equipment. In addition, it will also cause overheating of conductors and induction motors. Presence of harmonics cause erratic operation of the such sensitive devices. Also it will create unnecessary magnetic field near transformer and switch gears. These magnetic field adversely affect the performance transformer, switch gears. Therefore it is necessary to reduce the harmonics.

A three phase voltage source inverter is used. Pulse width modulation method is employed to increase the quality of the inverter. PWM methods are used to avoid the harmonics. Sine PWM and space vector PWM are the commonly used PWM methods. Out of these, Space Vector PWM is employed. Because only 66.5% of the square wave output is obtained in the Sine PWM method.

Maximum dc voltage that can be rectified from the three phase supply is 560 V. 372 V is only available at the inverter output stage. But most of the commercial motors and other equipments are rated above 400V. On the other hand, space vector PWM provide 74.3% of square wave output. As a result 416 V is supplied by the inverter. Hence higher amount of AC side voltage can be obtained with the same Dc bus voltage by space vector modulation. By adopting space vector PWM method, it is easy to meet the voltage requirement of the motors.

II. SPACE VECTOR CONCEPT

A. *Voltage SVPWM:*

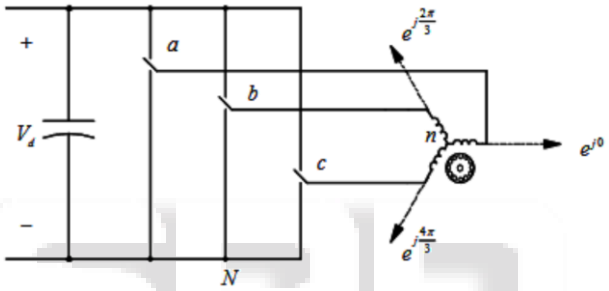

Fig. 1: Three-phase inverter.

The inverter in Fig. 1 has three switching power-poles, each consisting of a bi-positional switch either up or down. The object is to synthesize, by PWM, the average output of the inverter to be such that the desired balanced set of voltages vectors $\bar{v}_{an}(t)$, $\bar{v}_{bn}(t)$ and $\bar{v}_{cn}(t)$ appears across the load, be it a motor stator winding as shown in Fig. 1 for a counter clockwise rotation, or a UPS system, where $\bar{v}_{an}(t)$ + $\bar{v}_{bn}(t)$+ $\bar{v}_{cn}(t)$= 0. In terms of the desired phase voltages, the voltage space vector can be written by multiplying phase voltages by their phase orientations as,

$$\vec{v}_s(t) = \bar{v}_{an}(t)e^{j0} + \bar{v}_{bn}(t)e^{j2\pi/3} + \bar{v}_{cn}(t)e^{j4\pi/3}$$

In Fig. 1, in terms of the switching power-pole output voltages with respect to the negative dc bus,

$$\bar{v}_{an} = \bar{v}_{aN} + \bar{v}_{Nn,}\ \bar{v}_{bn} = \bar{v}_{bN} + \bar{v}_{Nn,}\ \bar{v}_{cn} = \bar{v}_{cN} + \bar{v}_{Nn}$$

Recognizing that $e^{j0} + e^{j2\pi/3} + e^{j4\pi/3} = 0$, and the voltage space vector can be written in terms of the switching power-pole average output voltages as the voltage space vector can be written in terms of the switching power-pole average output voltages as

$$\vec{v}_s(t) = \bar{v}_{aN}(t)e^{j0} + \bar{v}_{bN}(t)e^{j2\pi/3} + \bar{v}_{cN}(t)e^{j4\pi/3}$$

A switch in a switching power-pole of Fig. 1 is either up or down, with the instantaneous output voltage either 1 or 0 times V_d with three poles, eight switch status combinations are possible. The voltage space vector can instantly take on one of the following seven distinct instantaneous values as shown in Table 1, where phase "a" is represented by the least significant digit and phase "c" by the most significant digit.

Switch State			Basic Vector	Value
c	b	a		
0	0	0	$\vec{v}_0(000)$	0
0	0	1	$\vec{v}_1(001)$	$V_d e^{j0}$
0	1	0	$\vec{v}_2(010)$	$V_d e^{j\frac{2\pi}{3}}$
0	1	1	$\vec{v}_3(011)$	$V_d e^{j\frac{\pi}{3}}$
1	0	0	$\vec{v}_4(100)$	$V_d e^{j\frac{4\pi}{3}}$
1	0	1	$\vec{v}_5(101)$	$V_d e^{j\frac{5\pi}{3}}$
1	1	0	$\vec{v}_6(110)$	$V_d e^{j\pi}$
1	1	1	$\vec{v}_7(111)$	0

Table 1: Instantaneous Basic Voltage Vectors.

In Table 1, $\vec{v}_0$ and $\vec{v}_7$ are the zero vectors because of their values. The resulting instantaneous voltage vectors, which we will call the basic vectors, are shown in Fig. 2a forming six sectors. The average voltage vector is synthesized by time-weighted averaging of the two adjacent basic non-zero voltage vectors that form the sector (in which the average voltage vector to be synthesized lies) but using both the zero vectors of equal duration. We will begin by synthesizing the average voltage vector in sector 1, as shown in by $\vec{v}_s(t)$ in Fig. 2b. The adjacent basic vectors $\vec{v}_1$ and $\vec{v}_3$ are applied for intervals xT_s and yT_s respectively, and the zero vectors $\vec{v}_0$ and $\vec{v}_7$ are applied for a duration $z/2\ T_s$ each. By time weighted averaging,

$$v_s(t) = \frac{1}{T_s}[xT_s v_1 + yT_s v_3 + zT_s 0] = xv_1 + yv_3$$

Where x + y + z =1.Expressing the basic vectors in terms of their amplitude and phase angles results in,

$$\vec{v}_s(t) = \hat{V}_s e^{j\theta_s}(t) = V_d(xe^{j0} + ye^{j\pi/3})$$

From Fig. 2b, and equation for $\vec{v}_s(t)$ it is clear that the ratio y/x dictates the orientation θ_s, and introducing the zero-voltage interval $z = (1 - x - y)$ controls the amplitude $\hat{V}_s$. At the limit, where $z = 0$ and hence, $x + y = 1$, the tips of the voltage space vectors lie on the straight line connecting the two non-zero basic vectors in Fig. 2b. However, normally the three voltages to be synthesized vary sinusoidally in time, resulting in a rotating voltage space vector $\vec{v}_s(t)$ of constant amplitude. At the limit, shown by the dashed circle in Fig 2b this amplitude has a maximum value,

$$(\hat{V}_s)_{max} = V_d \cos\left(\frac{\pi}{6}\right) = \frac{\sqrt{3}}{2} V_d$$

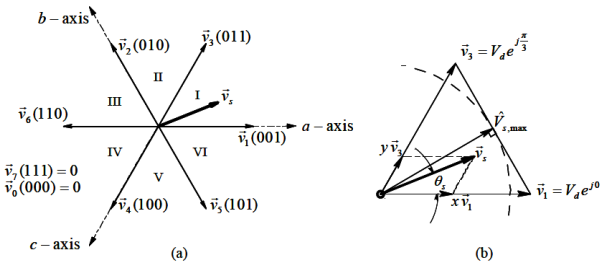

Fig. 2: Instantaneous basic vectors and synthesis of $\vec{v}_s(t)$.

Therefore the corresponding phase voltage peak, 2/3 times the space vector peak, has the following maximum from

$$(\hat{V}_a)_{max} = \frac{1}{\sqrt{3}} V_d$$

In Sine-PWM $(\hat{V}_a)_{max} = \frac{1}{2} V_d$. Therefore, comparing that with above equation shows that the SV-PWM results in a higher limit on the available output voltage by a factor of $2/\sqrt{3}$, or by approximately 15 percent.

B. Carrier Based Implementation of SVPWM:

In general, in a carrier-based PWM as shown in Fig. 3a, a control voltage is compared with a high frequency carrier signal of a triangular waveform that establishes the switching frequency f_s of the inverter. The resulting output voltage in Fig. 3 b has an average value that depends on the control voltage;

$$\overline{v}_{aN}(t) = \frac{V_d}{2} + \frac{V_d}{2}\frac{v_{control,a}\ (t)}{\hat{V}_{tri}}$$

Similar expressions hold for the average outputs of the other two poles in terms of their respective control voltages. These expressions lead to an average representation as shown in Fig. 3c for each pole as the sum of the desired phase voltage and a common-mode voltage $\overline{v}_{cm}(t)$as discussed below.

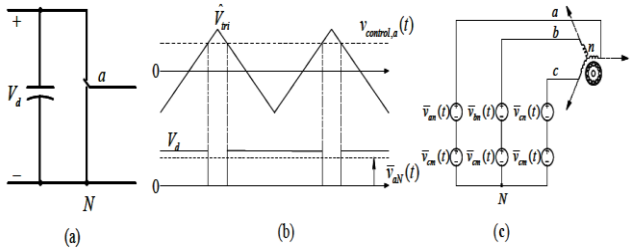

Fig. 3: (a) Switching power-pole, (b) carrier-based PWM, (c) average power-pole output.

In Sine-PWM, the control voltages form a balanced sinusoidal set of signals such their instantaneous sum is always zero. Therefore, they have no common-mode voltage, and the average voltage of each pole has a common-mode voltage $\overline{v}_{cm}(t) = 0.5V_d$

In SV-PWM, Note from Fig. 2b that in sector 1 with the non-zero basic vectors $\vec{v}_1(001)$ and $\vec{v}_3(011)$, the instantaneous power-pole "*c*" voltage is always 0 except it is V_d for a $\frac{z}{2}\ T_s$ interval corresponding to $\vec{v}_7(111)$. Therefore, the average value of the power-pole "c" output is $\overline{V}_{cN}(t) = \frac{z}{2}V_d$.

Also from Fig. 2b, in sector 1 with the non-zero basic vectors $\vec{v}_1(001)$ and $\vec{v}_3(011)$, switching-pole "*a*" voltage is always 0 except it is V_d for a $\frac{z}{2}\ T_s$ interval corresponding to $\vec{v}_0(000)$. Therefore, the average value of the power-pole "a" output is $\overline{V}_{aN}(t) = V_d - \frac{z}{2}V_d$.

$$\overline{v}_{cn}(t) + \overline{v}_{cm}(t) = \frac{z}{2}V_d$$

and

$$\overline{v}_{an}(t) + \overline{v}_{cm}(t) = V_d - \frac{z}{2}V_d$$

From the above two equation using the fact that $\vec{v}_{an}(t) + \vec{v}_{bn}(t) + \vec{v}_{cn}(t) = 0$

$$\overline{v}_{cm}(t) = \frac{1}{2}V_d + \frac{\overline{v}_{bn}}{2}(t)$$

This is valid only for sector 1. To generalize to all sectors $\overline{v}_{bn}(t)$ can be replaced by the maximum and minimum of the phase voltages as follows:

$$\overline{v}_{cm}(t) = \frac{1}{2}V_d + \left(\frac{\max(\overline{v}_{an},\overline{v}_{bn},\overline{v}_{cn}) + \min(\overline{v}_{an},\overline{v}_{bn},\overline{v}_{cn})}{2}\right)$$

$$\frac{v_{control,a}(t)}{\hat{V}_{tri}} = \frac{\overline{v}_{an}(t)}{\frac{V_d}{2}} - \left(\frac{\max(\overline{v}_{an},\overline{v}_{bn},\overline{v}_{cn}) + \min(\overline{v}_{an},\overline{v}_{bn},\overline{v}_{cn})}{V_d}\right)$$

In Sine-PWM, the second term in the right side of above equation is zero. The limits of Sine-PWM and the SVPWM schemes are shown in Fig. 4a by their space vector circles, and the corresponding control voltages are shown in Fig. 4b. This figure clearly shows the benefit of using SV-PWM over Sine-PWM leading to higher utilization of the dc-bus voltage. The above discussion also shows that the SV-PWM can be implemented as simply as the Sine-PWM using carrier-based pulse-width modulation.

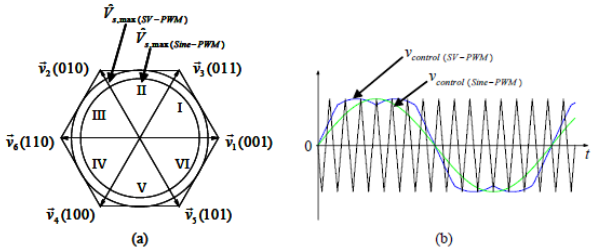

Fig. 4: Limits of SV-PWM and Sine-PWM.

III. INDUCTION MOTOR MODEL

Reference frame are very much like observer platforms, in that each of the platforms gives a unique view of the system at hand as well as a dramatic simplification of the system equation. For example, for the purpose of control, it is desirable to have the system variables as dc quantities, although the actual variables are sinusoidal. This could be accomplished by having a reference frame revolving at the same angular speed as that of the sinusoidal variable. As the reference frames are moving at an angular speed equal to the angular speed equal to angular frequency of sinusoidal supply, so that differential speed between them is reduced to zero, resulting in the sinusoid signal behaving as DC signal from the reference frames. So by moving that lane, it becomes easier to develop a small-signal equation out of a non-linear equations, as the operating point is described only by DC values; this then leads to linearised system around operating point. Such advantages are many from using reference frames, instead of deriving the transformation for each and every particular reference frame; it is advantageous to derive general transformation for an arbitrary rotating reference. frame. Then any particular reference frame model can be derived by substituting the appropriate frame speed and position in the generalized reference model.

The voltage equations in arbitrary reference frame in expanded form is as follows

$$v_{qs} = r_s i_{qs} + \omega\lambda_{ds} + p\lambda_{qs}$$
$$v_{ds} = r_s i_{ds} - \omega\lambda_{qs} + p\lambda_{ds}$$
$$v_{0s} = r_s i_{0s} + p\lambda_{0s}$$
$$v_{qr}' = r_r' i_{qr}' + (\omega - \omega_r)\lambda_{dr}' + p\lambda_{qr}'$$
$$v_{dr}' = r_r' i_{dr}' - (\omega - \omega_r)\lambda_{qr}' + p\lambda_{dr}'$$
$$v_{0r}' = r_r' i_{0r}' + p\lambda_{0r}'$$

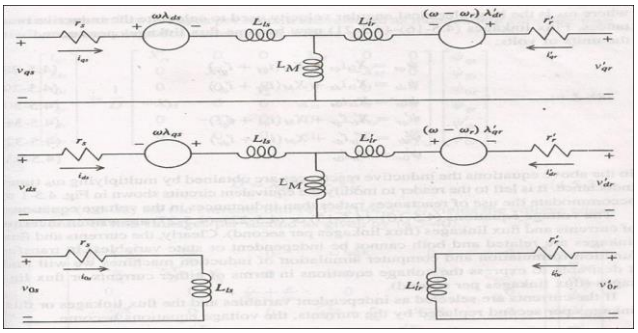

Fig. 5: Arbitrary reference- frame equivalent circuits for a 3 phase symmetrical IM.

$$\lambda_{qs} = L_{ls} i_{qs} + L_M(i_{qs} + i_{qr}')$$
$$\lambda_{ds} = L_{ls} i_{ds} + L_M(i_{ds} + i_{dr}')$$
$$\lambda_{0s} = L_{ls} i_{0s}$$
$$\lambda_{qr}' = L_{lr}' i_{qr}' + L_M(i_{qs} + i_{qr}')$$
$$\lambda_{dr}' = L_{lr}' i_{dr}' + L_M(i_{ds} + i_{dr}')$$
$$\lambda_{0r}' = L_{lr}' i_{0r}'$$

Because the machine and power system parameters are nearly always given in ohms or percent or per unit of a base impedance, it is convenient to express the voltage and flux linkages in terms of reactances rather than inductances.

$$v_{qs} = r_s i_{qs} + \frac{\omega}{\omega_b}\varphi_{ds} + \frac{p}{\omega_b}\varphi_{qs}$$
$$v_{ds} = r_s i_{ds} - \frac{\omega}{\omega_b}\varphi_{qs} + \frac{p}{\omega_b}\varphi_{ds}$$
$$v_{0s} = r_s i_{0s} + \frac{p}{\omega_b}\varphi_{0s}$$
$$v_{qr}' = r_r' i_{qr}' + \frac{\omega - \omega_r}{\omega_b}\varphi_{dr}' + \frac{p}{\omega_b}\varphi_{qr}'$$
$$v_{dr}' = r_r' i_{dr}' - \frac{\omega - \omega_r}{\omega_b}\varphi_{qr}' + \frac{p}{\omega_b}\varphi_{dr}'$$
$$v_{0r}' = r_r' i_{0r}' + \frac{p}{\omega_b}\varphi_{0r}'$$

Where ω_b is the base electrical angular velocity used to calculate the inductive reactance. Flux linkage become flux linkages per second with units of volts:

$$\varphi_{qs} = X_{ls} i_{qs} + X_M(i_{qs} + i_{qr}')$$
$$\varphi_{ds} = X_{ls} i_{ds} + X_M(i_{ds} + i_{dr}')$$
$$\varphi_{0s} = X_{ls} i_{0s}$$
$$\varphi_{qr}' = X_{lr}' i_{qr}' + X_M(i_{qs} + i_{qr}')$$
$$\varphi_{dr}' = X_{lr}' i_{dr}' + X_M(i_{ds} + i_{dr}')$$
$$\varphi_{0r}' = X_{lr}' i_{0r}'$$

The voltage equations are written in terms of current and flux linkages. If the currents are selected as independent variables and the flux linkages or flux linkages per second replaced by currents, the voltage equation become,

$X_{ss} = X_{ls} + X_M$

$$X_{rr}' = X_{lr}' + X_M$$

$$\begin{bmatrix} v_{qs} \\ v_{ds} \\ v_{0s} \\ v_{qr}' \\ v_{dr}' \\ v_{0r}' \end{bmatrix} = \begin{bmatrix} r_s + \frac{p}{\omega_b}X_{ss} & \frac{\omega}{\omega_b}X_{ss} & 0 & \frac{p}{\omega_b}X_M & \frac{\omega}{\omega_b}X_M & 0 \\ -\frac{\omega}{\omega_b}X_{ss} & r_s + \frac{p}{\omega_b}X_{ss} & 0 & -\frac{\omega}{\omega_b}X_M & \frac{p}{\omega_b}X_M & 0 \\ 0 & 0 & r_s + \frac{p}{\omega_b}X_{ls} & 0 & 0 & 0 \\ \frac{p}{\omega_b}X_M & \frac{\omega - \omega_r}{\omega_b}X_M & 0 & r_r' + \frac{p}{\omega_b}X_{rr}' & \frac{\omega - \omega_r}{\omega_b}X_{rr}' & 0 \\ -\left(\frac{\omega - \omega_r}{\omega_b}\right)X_M & \frac{p}{\omega_b}X_M & 0 & -\left(\frac{\omega - \omega_r}{\omega_b}\right)X_{rr}' & r_r' + \frac{p}{\omega_b}X_{rr}' & 0 \\ 0 & 0 & 0 & 0 & 0 & r_r' + \frac{p}{\omega_b}X_{lr}' \end{bmatrix} \begin{bmatrix} i_{qs} \\ i_{ds} \\ i_{0s} \\ i_{qr}' \\ i_{dr}' \\ i_{0r}' \end{bmatrix}$$

IV. SIMULATION RESULTS

A. SVPWM Inverter

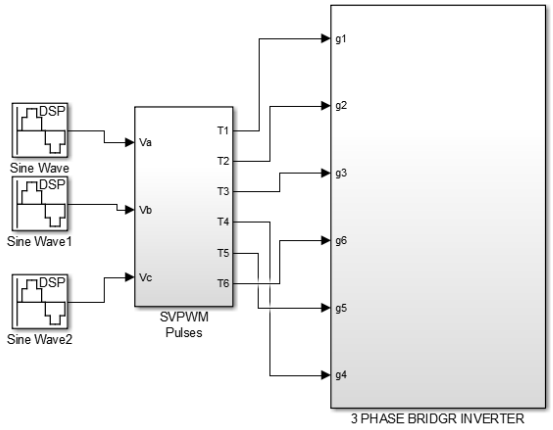

Fig. 6: SVPWM inverter

Above figure shows the SIMULINK model of SVPWM controlled bridge inverter. Three phase supply which are 120^0 apart are given to the SVPWM block in which space vector switching signal is generated. In the final block generated switching signal is applied to the VSI switches.

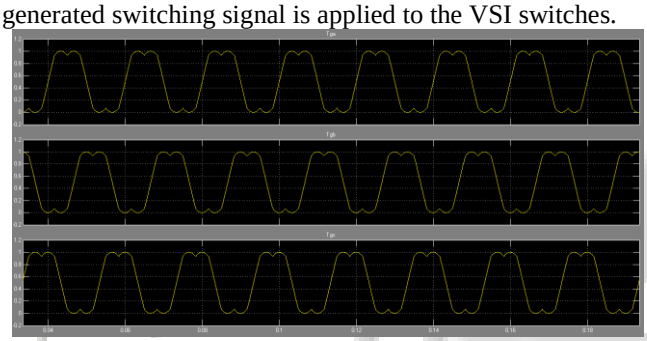

Fig. 7: Reference voltage waveform of SVPWM.

In the embedded MATLAB function the SVPWM algorithm has been written, creating necessary space vector signal. Then this space vector signal has been compared with the triangular carrier wave and required switching pulse has been generated. Switching pulses generated is applied to the six switches of the voltage source inverter.

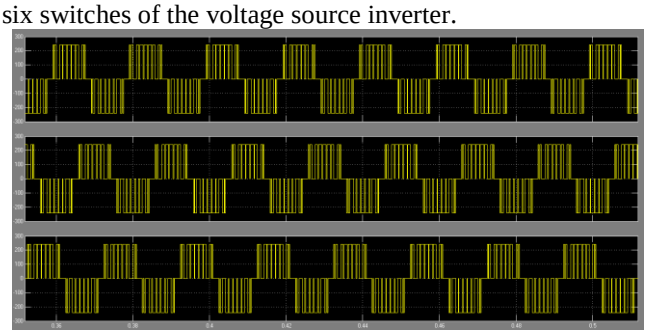

Fig. 8: Output voltage

V. MODEL

HP Rating	3
Volts	220
rpm	1710
r_s	0.435Ω
X_{ls}	0.754Ω
X_M	26.13Ω
r_r'	0.816Ω
X_{lr}'	0.754Ω
J	0.089kg.m^2

Table 2 Motor Parameters.

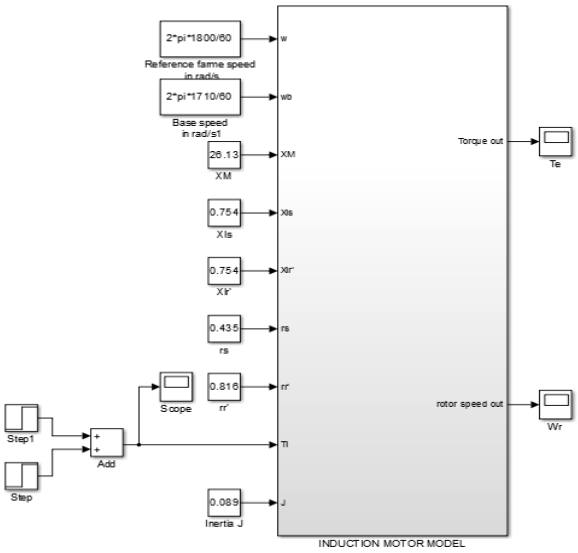

Fig. 8: IM model

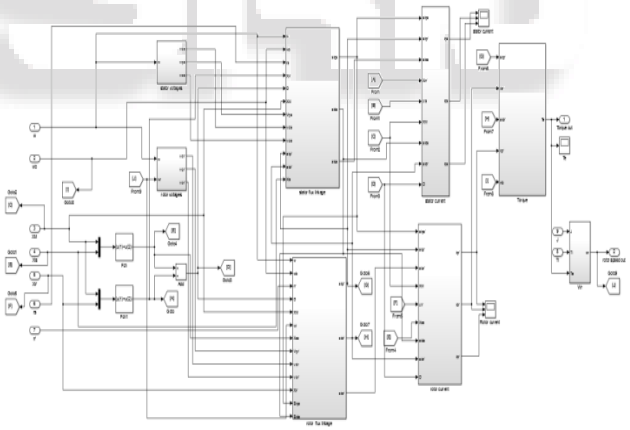

Fig. 9: IM model

The Fig. 8 & 9 shows the model of induction motor in MATLAB/Simulink. The parameters of machine are shown in table 2.

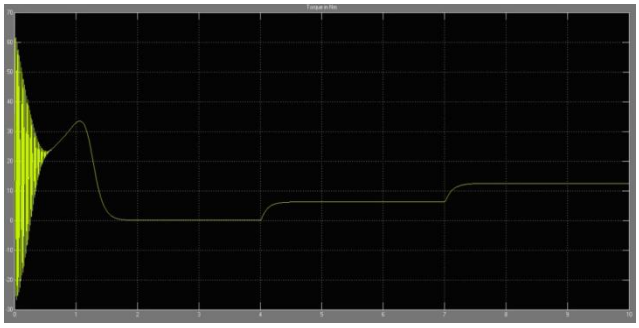

Fig. 10: Electromagnetic torque.

The Fig. 10 & 11 gives the torque and speed of induction motor respectively. The machine is initially stalled when rated balanced voltage is applied with $v_{as} = \sqrt{2}V_s cos wt$.

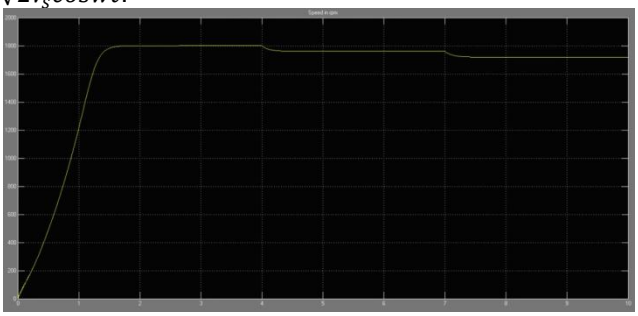

Fig. 11: Rotor speed ω_r

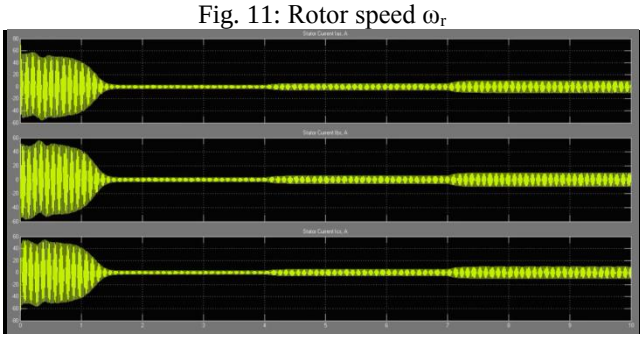

Fig. 12: Stator current.

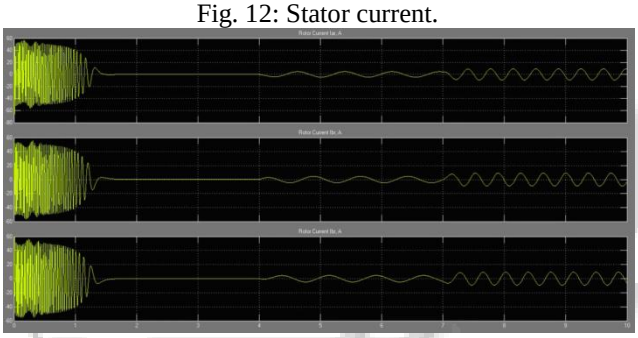

Fig. 13: Rotor current.

VI. Experimental Setup

The prototype of the 3 phase bridge inverter is setup in the laboratory and output voltage of inverter is measured using DSO. The gate pulses for the inverter is generated using Arduino Mega microcontroller board.

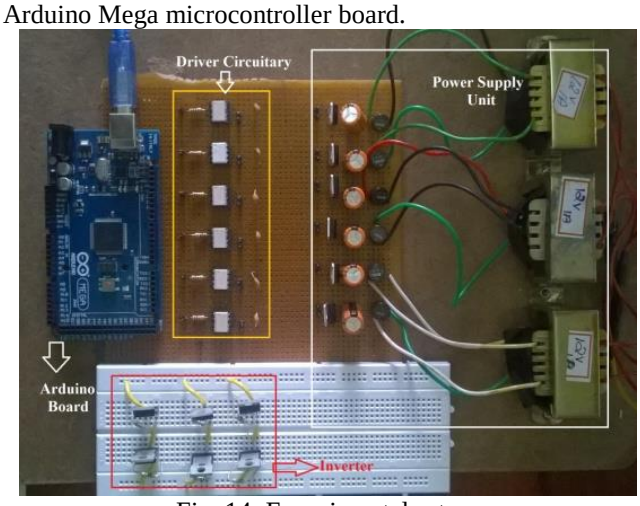

Fig. 14: Experimental setup.

The Fig. 14 shows the whole experimental setup. It has four different section Inverter section, Arduino Mega microcontroller board, Driver section, power supply unit.

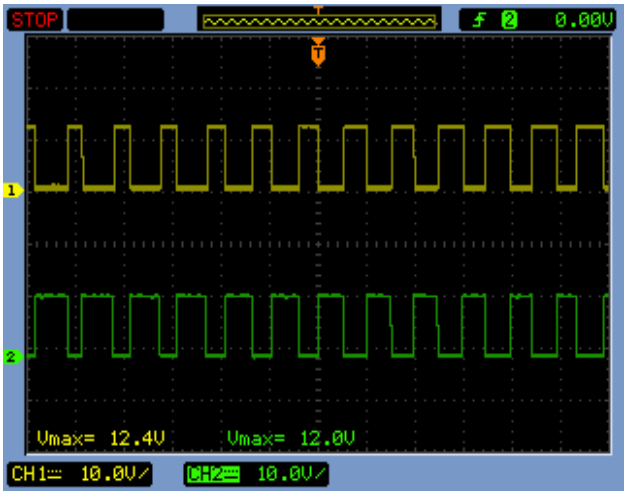

Fig. 15: Output of driver circuit (switching signal for S_1 and S_2).

The Fig. 16 shows the output line voltage obtained from the SVPWM inverter. The input voltage is given as $V_d = 5V$.

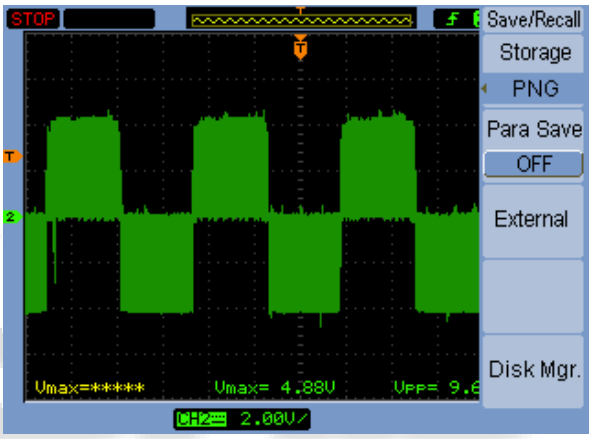

Fig. 16: Output voltage.

VII. Conclusion

Increasing trend of using space vector PWM (SVPWM) is because of their easier digital realisation and better DC bus utilisation. Firstly, model of a three-phase VSI is discussed based on space vector representation. The SVPWM results in a higher limit on the available output voltage by a factor 15%. The simulation model of SVPWM controlled inverter is obtained using MATLAB/SIMULINK. The prototype of 3 phase bridge inverter is setup and gate pulses are obtained from Arduino Mega2560. The dynamic analysis of the symmetrical induction machines in the arbitrary reference frame has been intensively used as a standard simulation approach from which any particular mode of operation may be then developed. MATLAB/SIMULINK has an advantage over other machine simulators in modelling the induction machines.

Acknowledgment

It is a great pleasure to acknowledge all those who have assisted and supported me for successfully completing the paper. I express my deep sense of gratitude to Asst. Prof. Jisha Kuruvilla P, for the valuable guidance as well as timely advice which helped me a lot in completing the paper successfully. I am deeply indebted to associate Prof. Beena

M Varghese, her guidance, patience and encouragement will be a guiding spirit in all endeavours of my future.

REFERENCES

[1] Navneet Kumar, Thanga Raj Chelliah, S.P. Srivastava,"Adaptive control schemes for Improving dynamic performance of efficiency optimized induction motor drives" *ISA Transactions* 2015.
[2] N. Mohan, " Advanced Electric Drives: Analysis, Control and Modelling using Simulink" *MNPERE* 2001.
[3] N. Mohan, "First Course on Power Electronics" *MNPERE* 2004.
[4] R Krishnan, "Electric motor drives, Modelling, Analysis and Control" *Prentice Hall of India* 2005.
[5] Paul C. Krause, Oleg Wasynczuk Scott D.Sudhoff, "Electric motor drives, Modelling, Analysis and Control" *IEEE Press Power Engineering Series* 2012.
[6] M. Chilikin,"Electric Drives"*MIR Publishers, Moscow* 1976.
[7] P S Bimbhra, "Power Electronics"*Khanna Publishers* 2011.
[8] G. Narayanan, and V. T. Ranganathan, "Two Novel Synchronized Bus- Clamping PWM Strategies Based on Space Vector Approach for High Power Drives" *IEEE Trans. Power. Electron* vol. 17, no. 1, pp. 8493, Jan. 2002.

